



ELSEVIER

Applied Surface Science 197–198 (2002) 100–106

applied  
surface science

www.elsevier.com/locate/apsusc

# On the white light luminescence induced by irradiation of sodium nitrate single crystals by 1064 nm laser light

Bandis<sup>1</sup>, L. Cramer, T.E. Holt, S.C. Langford, J.T. Dickinson\*

*Department of Physics, Washington State University, Pullman, WA 99164-2814, USA*

## Abstract

A number of wide bandgap inorganic materials can be prepared so that stimulation with nanosecond pulses of near infra-red (1064 nm—Nd:YAG fundamental) generates intense, transient white light. This light can span from 300 to 900 nm. Here, we characterize this emission from single crystal NaNO<sub>3</sub> and show that it is due to optical breakdown in the bulk. We contrast the behavior and character of time resolved spectra of this bulk breakdown with surface breakdown and provide evidence of defect mediated processes being responsible for the observed avalanche. We also conclude that confinement of the avalanche is essential for the production of this broad banded luminescence.

© 2002 Elsevier Science B.V. All rights reserved.

*PACS:* Laser materials, 42.70.H; Laser produced plasma, 52.50.J; Surface irradiation effects, 61.80.B; Defects Crystal, 61.72; Emission spectra-plasma, 52.25

*Keywords:* Luminescence; Sodium nitrate; Single crystals; Ionic crystal

## 1. Introduction

Transparent materials, such as ionic crystals, normally are expected to have weak interaction when exposed to relatively long wavelength laser light. However, defects can have a strong influence on laser materials interactions, particularly if occupied defect states couple to the radiation. In examining the interaction of nanosecond pulses of 1064 nm (Nd:YAG) radiation with the surfaces of materials such as NaNO<sub>3</sub>, MgO, NaCl, and SiO<sub>2</sub> (all highly transparent at

1064 nm) we found that under relatively mild focusing into the bulk of the material led to intense white light emission. In this paper, we describe this emission and show that it is due to confined optical breakdown.

Here, we focus our attention on single crystal sodium nitrate (NaNO<sub>3</sub>). NaNO<sub>3</sub> is a major component of high level nuclear wastes in underground storage tanks associated with US plutonium production during the cold war. Analyzing such wastes safely and accurately requires methods that do not involve direct contact, leading to techniques that utilize laser ablation and/or desorption, which are currently under development.

Sodium nitrate is a molecular-ionic crystal with a hexagonal unit cell and cleavage plane along the 10 $\bar{1}$ 4 direction, which intersects the c-axis at an angle of 43° 49' [1,2]. The absorption spectra of NaNO<sub>3</sub> show broad bands due to  $\pi^* \leftarrow \pi$  transitions which peak at  $\sim 6.4$  eV, and at  $\sim 10.5$  eV as well as  $\sim 12.1$  eV due

\* Corresponding author. Tel.: +1-509-335-4914; fax: 1-509-335-7816.

E-mail addresses: bandis@eim.org.gr (Bandis), jtd@wsu.edu (J.T. Dickinson).

<sup>1</sup> Present Address: Hellenic Institute of Metrology, Industrial Area of Thessaloniki, Block 45, Sindos, Thessaloniki 57022, Greece.

to transfer of charge into the sodium cationic states [1]. A much weaker band at  $\sim 4.2$  eV due to  $\pi^* \leftarrow n$  also has been observed; although it has 1000 times weaker oscillator strength, it can be of importance in experiments with high power lasers.

Although  $\text{NaNO}_3$  has intrinsic absorption bands neither at 248 nm nor at 1064 nm [1,2], it has been shown that exposing  $\text{NaNO}_3$  surfaces to either 248 nm (5 eV) KrF excimer laser or 1064 nm (1.16 eV) Nd:YAG laser radiation results in the emission of neutral atoms and molecules, positive ions, and electrons [3–7]. The observation of intense, highly localized, laser-induced visible radiation from dielectrics is associated with the presence of hot plasma, and often is used as a criterion for the occurrence of optical breakdown and the initiation of irreversible damage. Efforts to improve the chemical analysis and characterization techniques that utilize laser ablation and/or desorption, as well as the search for and development of optical components with as high as possible damage thresholds requires detailed understanding of the mechanisms involved when materials are exposed to near-threshold laser radiation. While making several laser induced particle emission measurements on single crystal sodium nitrate ( $\text{NaNO}_3$ ) we noticed at higher frequencies flashes of “white light” coming from inside the sample when irradiated with 1064 nm Nd:YAG laser light. Since this light spanned well above the photon energy of the laser light (1.16 eV) we were initially surprised to see it. Here, we explore the character of this broadband emission, compare its properties and behavior with light emitted from surface breakdown, and show that confinement of the breakdown is a major factor in generating this broadband emission.

## 2. Experiment

Our experiments were performed on cleaved melt grown  $\text{NaNO}_3$  single crystals. The crystals were grown in our laboratory after heating to 315 °C in air 99.0% pure  $\text{NaNO}_3$  powder (melting point: 306.8 °C) and then slowly, over a period of several days, cooling it back down to room temperature. A Continuum Sure-Light II Nd:YAG laser with a pulse width of  $\sim 8$  ns (FWHM) at 1064 nm was used for sample irradiation. The spectra of the emitted radiation were obtained using a TVC Jarrell-Ash MonoSpec 18 spectrograph

with a 150-g/mm grating, blazed at 450 nm and a Princeton Instruments intensified CCD (ITEA/CCD-576G/RBE). The intensity versus time of the visible part (300–800 nm) of the radiation was obtained using a 1 ns silicon photodiode behind a KG-5 Schott glass filter. A second photodiode behind a long pass RG-850 Schott glass filter (cutoff at 850 nm) was also used to monitor the time evolution of the laser intensity. The experiments were performed both in air and in a vacuum chamber with base pressure  $< 1 \times 10^{-7}$  Pa.

The confinement of the surface was accomplished by bonding freshly cleaved  $\text{NaNO}_3$  to a soda lime glass slide using epoxy adhesives. Two types of epoxy were used: UV curable and 5 min Epoxy. Epoxies, etc. manufactured the UV curable Type 60-7012 UV Curable Resin. These samples were exposed to a mercury vapor lamp for 6 h and left overnight. ITW Devon manufactured the 5 min epoxy; these samples were allowed to cure overnight in air. Both samples gave similar emissions from the confined interface.

## 3. Results and discussion

In Fig. 1(a) we show the image of the visible radiation emitted from the  $\text{NaNO}_3$  due to 1064 nm laser radiation ( $1.9 \text{ J/cm}^2$ ). The image of the 2.5 mm laser spot obtained with the same magnification is also shown for comparison in Fig. 1(b). The emitted radiation appears to the naked eye as white light highly localized to sub-mm spots within the laser path, indicating that it originates from specific, defect rich sites. Similar experiments with much thicker crystals demonstrate that the emission sites can be at the surface as well as in the bulk of the crystal. The intensity of the visible radiation rapidly depletes with increasing number of pulses; it takes less than 10 laser pulses even at fluences well above the single pulse damage threshold for the visible radiation to completely disappear. The white light is accompanied by permanent material damage. Such damaged spots are easy to detect when high laser fluences are involved, but with difficulty when near-threshold fluences are used. Damage at emission sites along confined surfaces is readily visible in SEM images. The presence of high defect densities is not required for the confined surface experiments since we increased the fluence to insure surface damage at the interface.

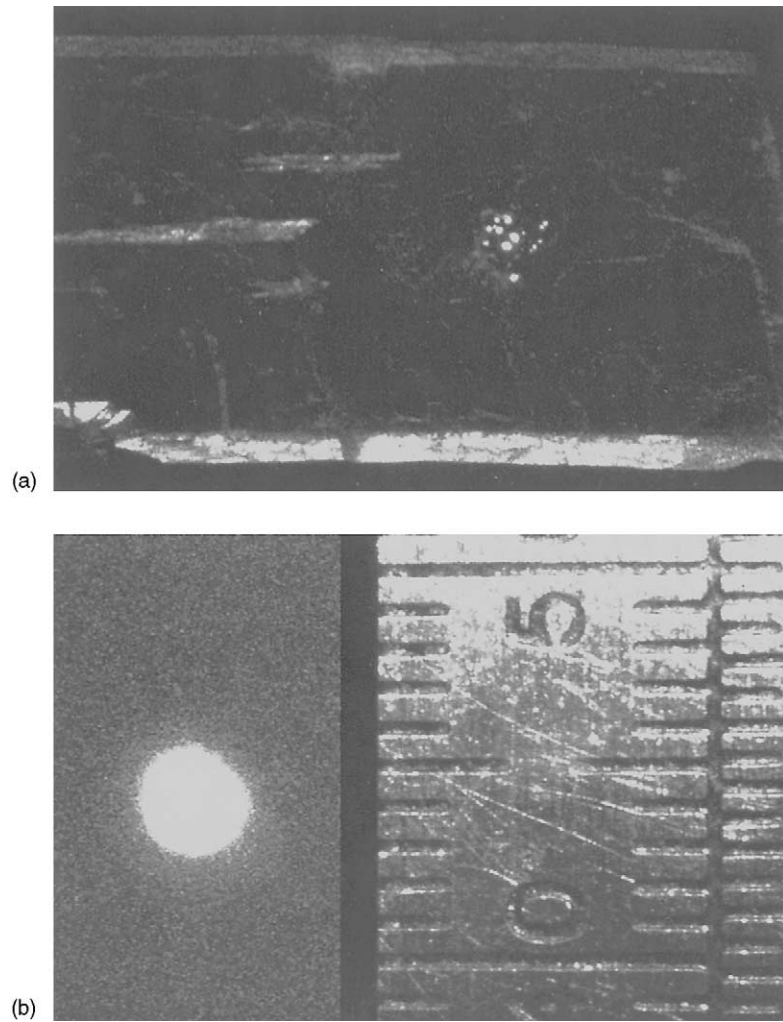


Fig. 1. Image of the highly localized visible radiation emitted from the  $\text{NaNO}_3$  due to 1064 nm laser radiation (a). The image of the 2.5 mm laser spot obtained with the same magnification is also shown for comparison (b).

We are not always able to correlate visible flaws in the bulk to white light emission.

The spectrum of the emitted visible radiation from bulk emission sites is shown in Fig. 2 (laser fluence  $\sim 2 \text{ J/cm}^2$ ). Our experiments find that, when the emission site is in the bulk of the crystal, the observed spectra are broad without any sharp atomic lines. In Fig. 2, we also see that there is a short wavelength cutoff at about 320 nm. Comparison of the emission spectra with the transmittance spectrum demonstrates that the cutoff is due to  $\text{NaNO}_3$  bulk absorption from the  $\pi^* \leftarrow n$  absorption band at  $\sim 4.2 \text{ eV}$  [8].

Sharp atomic lines are present when the emission sites are near/at the surface and a plume is observed (Fig. 3) in vacuum. At short time delays (top curve), the broadband emission is also seen and the short wavelength cutoff of this emission indicates that the broad visible radiation still originates from sites near but below the surface. When the onset of spectra acquisition is delayed more than about 200 ns after the laser pulse, the broad visible band is not observed. Only the sharp atomic lines (Na D lines) remain. Thus, the broad visible band decays relatively fast, while the atomic lines can easily last several microseconds even in vacuum, the latter due to electron collisions with

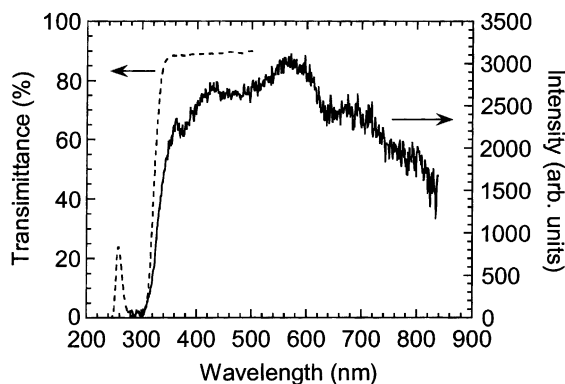


Fig. 2. Spectrum of the visible radiation emitted from a  $\text{NaNO}_3$  bulk emission sites upon exposure to 1064 nm laser radiation with fluence near the single pulse damage threshold. The absence of emission at wavelengths lower than 350 nm is consistent with absorption from the crystal surrounding the emission sites. Also note the absence of any sharp peaks due to atomic emission.

neutrals creating excited atoms [9,10]. Furthermore, this bulk-like, confined breakdown appears to be the only source of continuum white light; i.e. the plume itself is *not* the source of the continuum (which may help interpret a number of previously reported LIBS spectra from irradiated insulators).

The intensity of the broad visible band from bulk emission sites as measured with a 1 ns silicon photo-

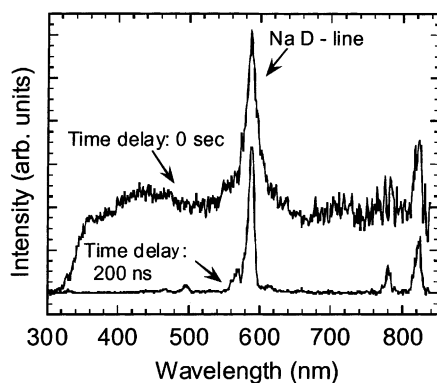


Fig. 3. Spectra of the visible radiation emitted from near surface emission sites of a  $\text{NaNO}_3$  single crystal upon exposure to 1064 nm laser radiation in vacuum. In addition to the broadband visible radiation, emission from atomic lines (Na ID) is also observed indicating the presence of plume. The emission due to Na, consistent with plume formation and in contrast with the broad band, decays much slower, in a time scale, which in vacuum, can be of the order of several microseconds.

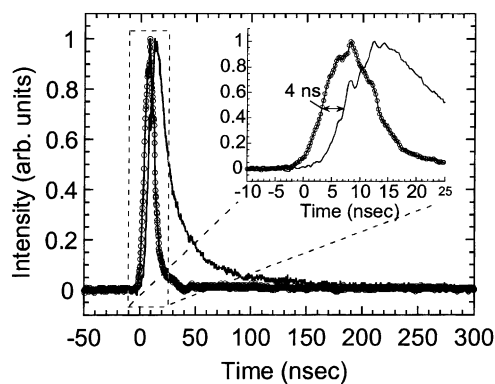


Fig. 4. Time evolution of the broad visible band from bulk emission sites (solid line). The emission intensity rises with a delay of a few nanoseconds with respect to the laser pulse (see inset) and typically decays in less than 200 ns. These data were acquired at a fluence of  $10 \text{ J/cm}^2$  using a short focal length lens focused well below the sample surface.

diode is plotted in Fig. 4 (solid line), and is compared with that of the laser pulse. The emission intensity rises with a delay of a few nanoseconds ( $\sim 4$  ns) with respect to the laser pulse (see inset in Fig. 4) and typically decays in less than 200 ns due to rapid cooling of the confined plasma. Pulses with higher emission intensity exhibit typically shorter delays ( $\leq 2$  ns) indicating that the observed delay depends on the absorbed energy, and therefore on the laser fluence as well as the defect density at the emission sites. At lower fluences we typically observe longer delays ( $\sim 5$  ns), which demonstrate that the initial electron density necessary for the plasma formation, is *not* due to a multiphoton absorption mechanism. In contrast, the observed delays are better explained assuming that electrons are raised from defect energy levels to the conduction band via successive single-photon absorption events. In such a sequence, electrons from the deep lying defect energy levels are raised to higher empty ones and from there to the conduction band [7,9,10]. As soon as the necessary electron density is available, the laser radiation is more efficiently absorbed resulting in the avalanche production of the plasma that emits the observed visible radiation.

The spectra shown in Figs. 2, 3 and 5, is plasma radiation emitted from bulk emission sites and exhibits broad features without any sharp atomic emission lines. This is due to the relatively high pressures and temperatures present in confined plasmas [11],

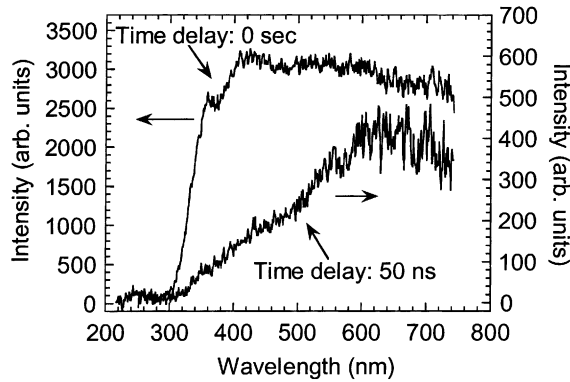


Fig. 5. Emission spectra from sites in the bulk of  $\text{NaNO}_3$  for two different time delays with respect to laser pulse.

that result in strong broadening and/or complete quenching of the atomic line emission due to collisional de-excitation (non-radiative decay). Furthermore, in Fig. 5 we plot and compare the spectra obtained with zero and 50 ns delay with respect to laser pulse; again consistent with plasma emission, we observe that the high-energy side (low wavelength) of the spectra decays faster than the low energy side (“cooling” of the plasma).

Optical breakdown in  $\text{NaNO}_3$  resulting in plasma emission from sites in the bulk will occasionally exhibit an absorption band at wavelengths consistent with absorption from atomic sodium. This indicates the presence of cooler neutral sodium atoms surround-

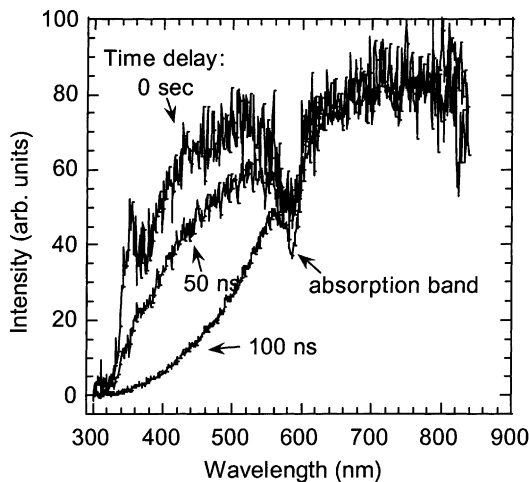
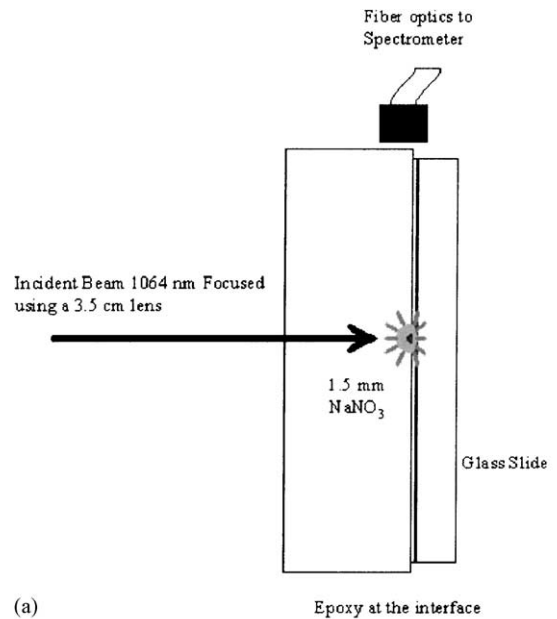
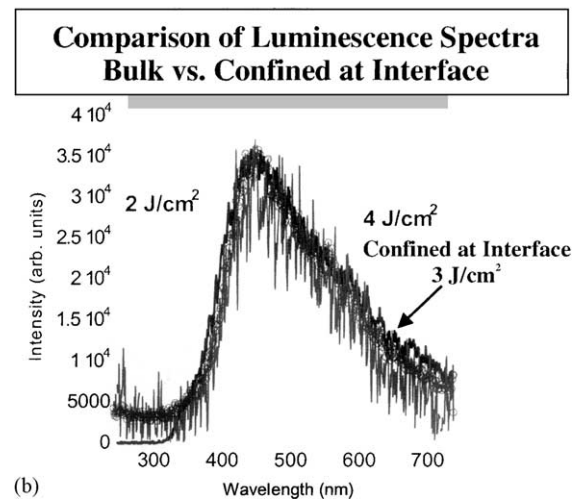


Fig. 6. Spectra from bulk emission sites that exhibit absorption due to neutral Na atoms. For comparison, we include the spectrum due to surface plume where a Na emission line is present (lower curve).

ing the hot plasma core. In Fig. 6, we show the spectra of such emission for 0, 50, and 100 ns delays with respect to the laser pulse. Similar to the spectra shown in Fig. 5, we observe that with increasing delays the high-energy emission site of the spectrum strongly decays faster indicating fast cooling of the plasma.



(a)



(b)

Fig. 7. (a) Arrangement for confining the free surface and observing the luminescence. (b) Comparison of uncorrected ‘white light’ spectra generated in the bulk of  $\text{NaNO}_3$  (at 2 and  $4 \text{ J/cm}^2$ ) with that generated at a confined interface (the  $\text{NaNO}_3$  surface and an epoxy cover). All three spectra are indistinguishable.

If the confinement of the plasma is essential for generating the white light spectrum, then configuring artificial confinement at a surface of the single crystal  $\text{NaNO}_3$  should generate white light. We found that simply clamping surfaces such as fused silica against the crystal did not provide sufficient confinement—Na rich plumes resulted when stimulated at 1064 nm. However, using a layer of a strong polymeric adhesive, such as an epoxy, generated the white light. Fig. 7(b) shows the uncorrected spectra of the broadband emission from the bulk (at two fluences) and the crystal-epoxy interface. As can be seen, there is no difference in the spectra. We attribute these similarities to the relatively high pressures and temperatures present in the confined case [11], which result in

extremely strong broadening and/or complete quenching of the atomic line emission due to collisional de-excitation (non-radiative decay). It should be noted that at higher fluence, Na D line on top of the white light could be generated at such an interface.

By carefully cleaving off the epoxy from the crystal, the irradiated regions of the interface can be examined. The SEM micrographs of such a confined surface are shown in Fig. 8(a) and (b) showing the damage caused by focusing the 1064 nm pulse at the crystal-epoxy interface. These damage sites were accompanied with white light only (no Na D line discernible). They show that the kernel or nucleus of the damage was at the surface of the crystal of  $\text{NaNO}_3$ . By simply providing the confinement of the adhesive, the formation of line spectra was totally inhibited.

#### 4. Conclusion

Exposure of single crystal  $\text{NaNO}_3$  to nanosecond pulses of 1064 nm radiation can lead to a broad band continuum that we have shown is due to highly localized, bulk, confined breakdown. The observed short wavelength cutoff in the emission spectra is due to bulk absorption of the material surrounding the emission sites. Study of the time evolution of the emitted radiation from bulk emission sites shows that, compared to plume radiation (emission from surface sites) that can last for microseconds, the broad visible band decays relatively fast in less than 200 ns due to rapid cooling of the confined plasma. The rise time of such radiation can exhibit delays up to several nanoseconds relative to the laser pulse, which demonstrates that the initial electron density, necessary for the plasma formation, is not due to multiphoton absorption. The observed delays can be understood assuming that initial excitation occurs via successive single-photon absorption events within clusters of defects which raise the electrons from deep lying defect energy levels to higher ones and from there to the conduction band [6,7]. Artificially confined substrates (using epoxy) generated the same spectra when breakdown occurred at the interface. Finally, surface breakdown was shown to yield continuum white light due to breakdown within the near surface bulk plus the usual atomic lines from the expanding plume due to electron collisions to create excited atoms.

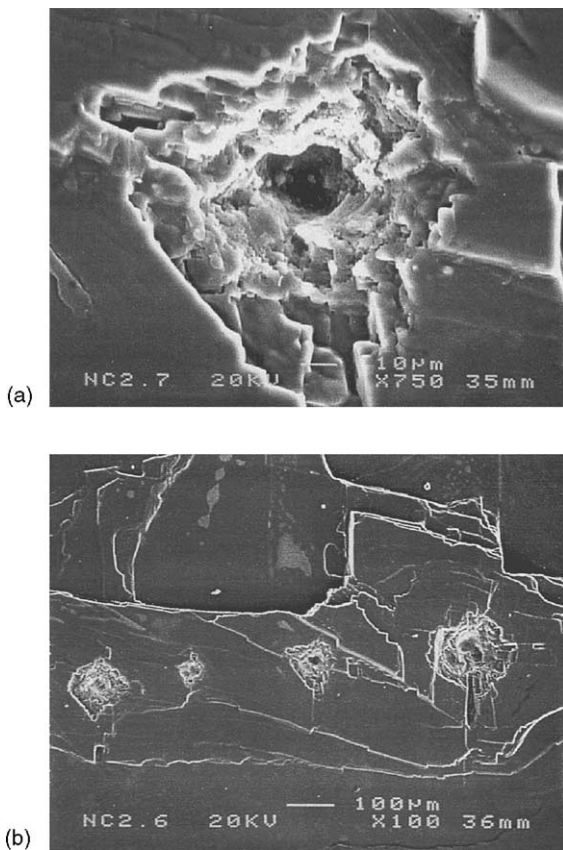


Fig. 8. (a) Single pulsed damage at confined interface as imaged with SEM. (b) SEM micrographs of single pulse damage of the confined interface at fluences below the threshold for the formation of Na D line emission.

## Acknowledgements

This work was supported by the Department of Energy under Contract DE-FG03-99ER14864 and an Equipment Grant from the National Science Foundation, DMR-9503304.

## References

- [1] H. Yamashita, R. Kato, *J. Phys. Soc. Jpn.* 29 (1970) 1557.
- [2] H. Yamashita, *J. Phys. Soc. Jpn.* 33 (1972) 1407.
- [3] R.L. Webb, S.C. Langford, J.T. Dickinson, *Nucl. Instrum. Meth. Phys. Res. B* 103 (1995) 297.
- [4] J.J. Shin, M.-W. Kim, J.T. Dickinson, *J. Appl. Phys.* 80 (1996) 7065.
- [5] D.R. Ermer, J.-J. Shin, S.C. Langford, K.W. Hipps, J.T. Dickinson, *J. Appl. Phys.* 80 (1996) 6452.
- [6] C. Bandis, S.C. Langford, J.T. Dickinson, *Appl. Phys. Lett.* 76 (2000) 421.
- [7] C. Bandis, S.C. Langford, J.T. Dickinson, D.R. Ermer, N. Itoh, *J. Appl. Phys.* 87 (2000) 1522.
- [8] M. Kamada, R. Kato, *J. Phys. Soc. Jpn.* 35 (1973) 1561.
- [9] D.R. Ermer, S.C. Langford, J.T. Dickinson, *J. Appl. Phys.* 81 (1997) 1495.
- [10] J.J. Shin, D.R. Ermer, S.C. Langford, J.T. Dickinson, *Appl. Phys. A* 64 (1997) 7.
- [11] D. Devaux, R. Fabbro, L. Tollier, E. Bartnicki, *J. Appl. Phys.* 74 (1993) 2268.